

## STABLE, HIGH QUANTUM EFFICIENCY, UV-ENHANCED SILICON PHOTODIODES BY ARSENIC DIFFUSION

RAJ KORDE<sup>1</sup> and JON GEIST<sup>2</sup>

<sup>1</sup>United Detector Technology, Hawthorne, CA 90250, U.S.A. and <sup>2</sup>National Bureau of Standards, Gaithersburg, MD 20899, U.S.A.

(Received 7 April 1986; in revised form 14 May 1986)

**Abstract**—Very high quantum efficiency, UV-enhanced silicon photodiodes have been developed by arsenic diffusion into *p*-type silicon as an alternative to the inversion layer photodiodes commonly used in precise radiometric and spectroscopic measurements. The fabricated diodes had an unbiased internal quantum efficiency that was 100% from 350 to 550 nm, and that exceeded 100% at shorter wavelengths. A typical responsivity at 200 nm was 0.1 A/W. No degradation in responsivity was detected anywhere in the 200–1100 nm range when these devices were exposed to 20 mW/cm<sup>2</sup> of 254 nm radiation for 60 days. Thus the theoretical maximum value of internal quantum efficiency for a diffused photodiode appears to have been achieved in the UV and short wavelength visible, without compromising the diode's long term stability. This is in marked contrast to older types of diffused photodiodes, which either were "dead" in the UV, or exhibited a spectral response vs flux characteristic that changed considerably with UV exposure.

### INTRODUCTION

Various aerospace, medical, spectroscopic and radiometric measurement applications require a semiconductor photodiode with high UV responsivity and long term stability. Many different types of silicon photodiode, such as Schottky barrier[1], extremely shallow diffused junction[2], natural inversion layer[3], double junction[4],  $n^+n^-p$ [5], and induced metallurgical junction[6] devices have been investigated for this application. Because the incident UV radiation is absorbed by silicon within a few tens of nanometers of the oxide-silicon interface, all of the above investigations included efforts to minimize recombination at and near this interface. However, it appears that 100% internal quantum efficiency has been achieved in the UV only with inversion layer diodes.

Inversion layer diodes have a low linearity range (the range over which the diode current is proportional to input irradiance) due to the inherently high sheet resistance of an inverted semiconductor layer. Also, there is some concern (for example, see Ref.[2]) that the oxide charge that sets up the inversion layer could be neutralized (in aerospace applications) by high energy particles, further reducing the already low linearity range.† Thus, there is a need for a diffused diode that is as responsive in the UV as the inversion layer diode, and is at least as stable under

UV radiation. Ideally the device would have a UV and short wavelength visible responsivity that was unaffected by x-rays, gamma rays and high energy particles, as well as by UV radiation.

### DESIGN CRITERIA

The design of a highly UV-responsive diffused diode dictates that the rate of recombination of photogenerated excess minority carriers in the diffused region and at the oxide-silicon interface be negligible compared to their rate of collection by the junction. This can be achieved with a "recombination-center free" diffused region, whose maximum dopant concentration is limited to avoid Auger recombination[7], and whose majority carrier profile creates a built-in field that repels excess minority carriers from the interface before they ever reach it.

The commonly used *p*-type impurity, boron, migrates from the silicon surface into the oxide during the final thermal oxidation step, which is carried out to grow a thin film of silicon dioxide that serves both to protect the silicon surface and as an antireflection coating. The resulting acceptor profile, which is depleted in the vicinity of the oxide-silicon interface, creates a built-in electric field perpendicular to the interface, directed toward the bulk. Any positive trapped oxide charge also contributes to this field, usually providing the dominant contribution very near the interface. The resulting electric field attracts the photo-generated minority carriers (electrons) created in the diffused region towards the oxide-silicon interface, greatly enhancing the carrier loss due to interface recombination[8,9]. This rules out the most

†We are able to produce inversion layer diodes that exhibit no linearity degradation at the ±0.5% level after exposure to 24 h of 1 mW/cm<sup>2</sup> of 254 nm radiation, but since different mechanisms are involved, we do not know whether these diodes would also be stable under exposure to high energy particles.

convenient  $p$ -type impurity for forming a  $p^+n$  UV enhanced photodiode by diffusion methods.

On the other hand,  $n$ -type impurities such as phosphorus and arsenic tend to pile up in the silicon during oxide growth, creating a built-in field near the oxide-silicon interface that is qualitatively similar to that existing in an inversion layer. Oxide- $n-p$  (opn) devices that use this built-in field to eliminate interface recombination have been proposed previously[10]. However, one of the authors (Jon Geist) failed in an attempt to achieve 100% internal quantum efficiency following the prescription outlined in Ref.[10]. A possible cause of this failure is that ion implantation damage remained after annealing, and reduced the front region lifetime to a level comparable to the collection time of the junction. In this paper, we describe devices similar to those proposed in Ref.[10], but in which every source of front region recombination is minimized.

Of the three most common  $n$ -type impurities, phosphorus, arsenic and antimony, it is arsenic that seems the most ideal. It has a zero misfit factor in silicon[11], which allows a considerable concentration of arsenic to be introduced into the silicon lattice without generating strain. Thus "recombination-center free" arsenic impurity diffusion can be achieved, provided that silicon with a sufficiently low concentration of dissolved oxygen is used as a starting material[12,13], and that slip and dislocation generation caused by temperature gradients are avoided during the high temperature wafer processing[14]. Additionally, the absence of lattice strain with arsenic diffusion avoids the flattening of the impurity profile near the silicon surface that occurs with boron, phosphorus, and antimony diffusion[15]. Finally, arsenic has a segregation coefficient comparable to that of phosphorus[16] and a thermal diffusion coefficient smaller than that of phosphorus[17], so the calculations mentioned in Ref.[10] should apply, at least qualitatively, to arsenic doped devices as well as to phosphorus doped devices.

#### DEVICE FABRICATION

Figure 1 is a schematic diagram of the type of device that we built to test the ideas presented in the last section. The starting material was a float-zone,  $\langle 111 \rangle$ ,  $p$ -type,  $110 \Omega \text{ cm}$ , one side mirror polished silicon wafer (Wacker Chemitronic†). After the  $p^+$  channel stop and  $n^+$  guard ring were formed by selective boron and phosphorus diffusions, respectively, arsenic was predeposited in the  $1 \text{ cm}^2$  active area of the device using a planar arsenic

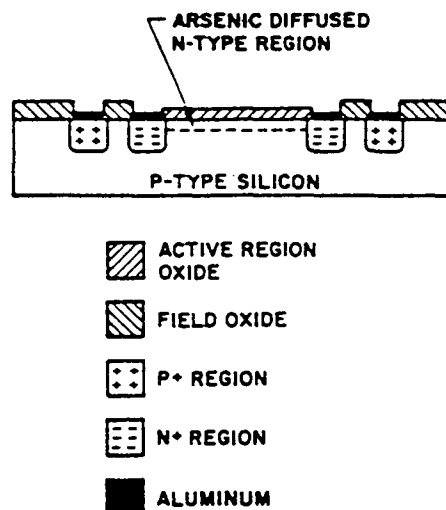


Fig. 1. Schematic diagram of the arsenic diffused UV-enhanced silicon photodiode.

source[18]. The arsenosilicate glass formed during the predeposition was etched in 10% hydrofluoric acid and the final passivating,  $\text{SiO}_2$ , anti-reflection coating was grown in dry oxygen. Windows were opened at the desired locations in the diffused regions by standard photolithographic processes, and aluminum was vacuum evaporated on these windows for ohmic contacts. The aluminum was sintered, and the wafers were sawed into the individual chips. The completed chips were mounted on standard UDT FIL UV-100 packages for performing the various electro-optical measurements described below.

#### RESULTS AND DISCUSSION

The spreading resistance profile for a typical arsenic diffused diode is shown in Fig. 2. No pile-up of arsenic at the oxide-silicon interface is evident from the profile, but spreading resistance may not have the sensitivity needed to detect this detail of the impurity profile. Very steep pile-up of phosphorus at the oxide-silicon interface after thermal oxidation has been observed[19] using Auger sputtering as a profiling technique. Since arsenic has a comparable segregation coefficient[16] and a smaller diffusion coefficient[17] than phosphorus, even steeper pile-up of arsenic can be expected. The high surface fields that pile-up generates are essential for the high UV quantum efficiency and stability desired of these diodes[9]. Indirect evidence for the actual occurrence of the pile-up is essentially the 100% internal quantum efficiency reported later in this paper.

A few obviously defective diodes were rejected on the basis of low shunt resistance or breakdown voltage. The shunt resistance of the remaining diodes, which was calculated as the average of the forward and reverse dark currents for a 10 mV bias voltage, clustered around  $40 \text{ M}\Omega$ . The breakdown voltage, which was measured on a transistor curve tracer,

†Reference in this paper to commercial products is provided to adequately describe the experimental technique. It implies neither indorsement by the National Bureau of Standards nor that the product so referenced is the best for the purpose.

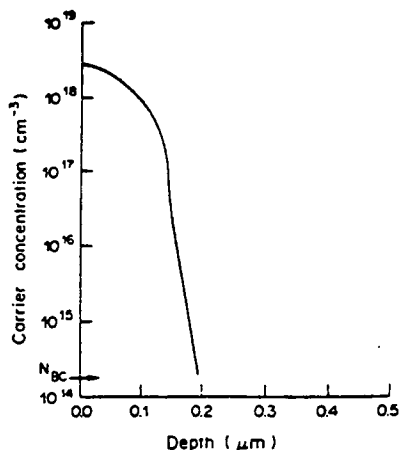


Fig. 2. Spreading resistance profile of the diffused arsenic.

clustered around 50 V, and the junction capacitance, which was measured with a capacitance bridge operating at 100 kHz, was found to cluster about 5 nF.

It is interesting to note that the capacitance of the arsenic diffused photodiodes is slightly higher than the capacitance of inversion layer photodiodes of the same active area fabricated on the same resistivity substrate. This is to be expected, because the capacitance of an inversion layer diode is the series combination of the depletion and inversion layer capacitances. Even though the arsenic diffused diodes had a higher junction capacitance, their 10–90% rise-time, which was about 2  $\mu$ s for 880 nm radiation, was about one half that of the equivalent inversion layer diode rise-time. The 880 nm rise-time could be further reduced either by fabricating the devices on higher resistivity substrates to reduce the junction capacitance, or by sacrificing visible region responsivity to diminish the carrier diffusion contribution to the rise-time, or by applying reverse bias.

The linearity range of the arsenic diffused diodes, which was measured at 633 nm using the a.c./d.c. method[20], extended from about 10 pW/cm<sup>2</sup> to about 1 mW/cm<sup>2</sup>. The upper end of this range is

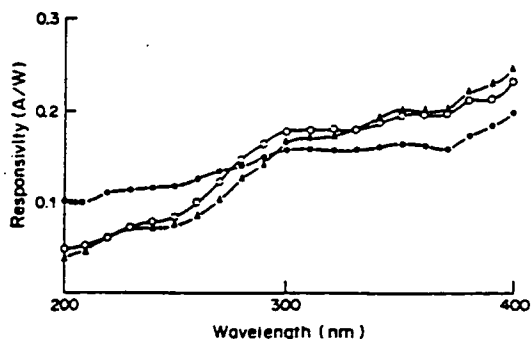


Fig. 3. UV region spectral responsivity of the arsenic diffused photodiode with 30 nm (●) and 55 nm (○) SiO<sub>2</sub> antireflection coatings. The responsivity of an inversion layer photodiode (▲) with a 55 nm SiO<sub>2</sub> antireflection coating is also shown for comparison.

about four times greater than that for the equivalent inversion layer diode.

Both the spectral responsivity in the 200–400 nm spectral region and the internal quantum efficiency in the 300–900 nm spectral region were measured on a few of the arsenic diffused devices. The UV spectral responsivity measurements were conducted by the comparison method[21] using a high spectral purity monochromator and a deuterium lamp UV source. The internal quantum efficiency measurements consisted of simultaneous measurements of diode reflectance[22] and spectral responsivity by the comparison method, using a different high spectral purity monochromator and an Argon mini-arc source. In both cases, the reference detector was a silicon photodiode whose absolute spectral responsivity had been determined independently at NBS.

Figure 3 shows the spectral responsivity of two typical arsenic diffused diodes having silicon dioxide antireflection coatings of 55 and 30 nm, respectively. The spectral responsivity of an inversion layer diode having a 55 nm silicon dioxide antireflection coating is also shown in Fig. 3 for comparison. As is evident from the figure, the inversion layer and arsenic doped devices with the same antireflection coating have essentially the same spectral responsivity, indicating minimal, if not negligible, recombination in the diffused region and at the interface.

Figure 4 shows the measured internal quantum efficiency of one of the arsenic diffused diodes from 300 to 600 nm. To the accuracy of this measurement, which varies from about  $\pm 0.5\%$  at 350 nm to about  $\pm 0.25\%$  at 550 nm, the internal quantum efficiency is unity in this wavelength range. The increase in internal quantum efficiency below 350 nm is caused by impact ionization involving energetic photo-generated carriers[23], while the decrease in internal quantum efficiency above 550 nm is caused by the recombination of some of the minority carriers created in the *p*-type silicon beyond the depletion region as described in Ref.[20].

Both the evidence of Fig. 4, and the fact that the responsivity of the arsenic diffused diode with the 30 nm antireflection coating is higher in the 200–220 nm region than that of any inversion layer device that we have previously measured, strongly suggest that recombination in the diffused region and at the oxide interface is indeed negligible in the arsenic diffused devices. This, in turn, suggests the existence of a strong built-in field at the oxide-silicon interface, which is consistent with arsenic redistribution pile-up during oxide growth.

The high internal quantum efficiency of the new arsenic diffused photodiodes will not be very useful if it is not stable under UV irradiation or if it decreases during storage. To test the stability of the fabricated devices under UV irradiation, they were continuously exposed to 20 mW/cm<sup>2</sup> of 254 nm radiation over a period of over 60 days, except for short periods when their spectral responsivity and linearity were re-

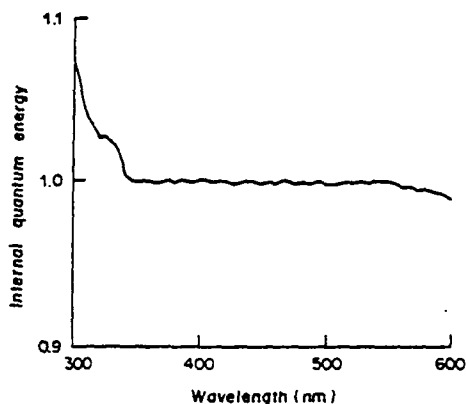


Fig. 4. Internal quantum efficiency of a typical UV-enhanced arsenic diffused photodiode.

measured. No degradation was observed in either characteristic at the  $\pm 0.5\%$  level of precision of our measurements during the entire duration of this experiment.

Recently, a decrease in UV responsivity during storage was reported for one type of UV enhanced photodiode[24], but such an experiment must last for a number of years before small trends can be detected. Perhaps valid accelerated aging tests can be developed, but they must also be validated against long term studies. So only time will tell if the devices described in this paper retain their high quantum efficiency over periods of many years. Certainly the results of the UV degradation studies are encouraging in this regard.

#### CONCLUSION

A new type of UV enhanced photodiode has been fabricated and tested. It was found to combine high UV quantum efficiency, linearity range and stability against exposure to intense UV irradiation.

*Acknowledgements*—We are grateful to Deepak Chopra of UDT for encouraging this work, to Berry Johnson and Gabe De Munda of Sohio Corporation for preparing the

arsenic predepositions for us, to Dick Duda of UDT for assisting with the spectral responsivity and linearity measurements, and to Bob Saunders and Jeanne Houston of NBS for the internal quantum efficiency measurements.

#### REFERENCES

1. S. S. Li, F. A. Lindholm and C. T. Wang, *J. appl. Phys.* **43**, 4123 (1972).
2. H. Ouchi, T. Makai, T. Kamei and M. Okamura, *IEEE Trans. Electron. Dev.* **ED-26**, 1965 (1979). (Including references therein.)
3. T. E. Hansen, *Physica Scripta* **18**, 471 (1978).
4. W. Munch, *Jap. J. Appl. Phys.* **16**, 271 (1977).
5. S. Chamberlain, *J. appl. Phys.* **50**, 7228 (1979).
6. R. Korde, *Proc. First Portland Int. Conf. on Silicon Materials and Technology*, (Abstract). Oregon State University, Portland (1985).
7. J. Dziejwior and W. Schmid, *Appl. Phys. Lett.* **31**, 346 (1977).
8. J. Geist, *J. appl. Phys.* **51**, 3993 (1980).
9. J. Verdebout, *Appl. Opt.* **23**, 4339 (1984).
10. J. Geist, E. Liang and A. R. Schaefer, *J. appl. Phys.* **52**, 4879 (1981).
11. S. K. Ghandi, *VLSI Fabrication Principles in Silicon and Gallium Arsenide*, p. 6. Wiley, New York (1983).
12. T. B. McGee, C. Leung, H. Kawayoshi, B. K. Furman and C. A. Evans, *Appl. Phys. Lett.* **39**, 413 (1981).
13. L. Jastrebski and P. Zanzucchi, In: *Semiconductor Silicon 1981*, p. 138. The Electrochemical Society (1981).
14. S. M. Hu, *Appl. Phys. Lett.* **22**, 261 (1973).
15. R. S. Korde, P. N. Goswami and M. S. Tyagi, *J. Inst. Electron. Telecomm. Engrs (India)* **25**, 251 (1979).
16. S. K. Ghandi, *VLSI Fabrication Principles in Silicon and Gallium Arsenide*, p. 173. Wiley, New York (1983).
17. S. M. Sze, *Physics of Semiconductor Devices*, p. 31. Wiley, New York (1969).
18. R. E. Tressler, H. J. Boglin, J. Monkowski, J. Stach, Gabe De Munda and C. Volk, *Solid-St. Techn.* **27**, 165 (1984).
19. S. A. Schwartz, R. W. Barton, C. P. Ho and C. R. Helms, *J. Electrochem. Soc.* **128**, 1101 (1981).
20. A. R. Schaefer, E. F. Zalewski and J. Geist, *Appl. Opt.* **22**, 1232 (1983).
21. W. Budde, *Optical Radiation Measurements, Vol. 4, Physical Detectors of Optical Radiation*, p. 39. Academic Press, New York (1983).
22. R. L. Booker and J. Geist, *Appl. Opt.* **23**, 1940 (1984).
23. J. Geist and C. S. Wang, *Phys. Rev.* **27**, 4841 (1983).
24. J. L. Gardner and F. J. Wilkinson, *Appl. Opt.* **24**, 1531 (1985).